A Markov reward process-based framework for resilience analysis of multistate energy systems under the threat of extreme events

Zhiguo Zeng, Yi-Ping Fang, Qingqing Zhai, Shijia Du

A Markov reward process-based framework for resilience analysis of multistate energy systems under the threat of extreme events

Zhiguo Zeng,[†] Yi-ping Fang,[†] Qingqing Zhai,[‡] Shijia Du (*)[§]

[†]Université Paris-Saclay, Chair on Risk and Resilience of Complex Systems, Laboratoie Genie Industriel, CentraleSupélec, 91190, Gif-sur-Yvette, France.

[‡]School of Management, Shanghai University, Shanghai 200444, China

[§]School of Reliability and Systems Engineering, Beihang University, 100191, Beijing, China.

Abstract

Energy systems are increasingly exposed to the threats of extreme events like floods, earthquakes and hurricanes. In practice, the behaviors of the systems affected by these extreme events are often modeled by multistate models to facilitate the analysis. In this paper, we develop a generic framework for resilience modelling and analysis of multistate energy systems. A multistate resilience model is developed based on a Markov reward process model, where the degradation and recovery of system performance are characterized by a continuous time discrete state Markov chain and the losses caused by the extreme event is modelled by the reward rates associated with the sojourns in the degradation states and the transitions among the states. Four numerical metrics are defined to describe different aspects of system resilience, *i.e.,* the resistant, absorption, recovery and overall resilience. A simulation-based algorithm is proposed for resilience analysis of multistate energy systems. The developed methods are applied for resilience modelling and analysis of a Nuclear Power Plant (NPP) under the threat of earthquakes. The Markov reward process model is developed following a probabilistic seismic hazard analysis, a fragility analysis and an event tree modelling of accident evolutions. Both a time-static and time-dependent resilience analysis are conducted and the results show that the developed model is able to comprehensively describe the resilience of multistate energy systems under the threats of extreme events.

Index Terms

Resilience, energy system, extreme events, multistate system, Markov reward model, accumulated reward.

* Email of the corresponding author: dushijia111@gmail.com

A Markov reward process-based framework for resilience analysis of multistate energy systems under the threat of extreme events

I. Introduction

Extreme events refer to the events that have high impacts but low occurrence probability, *e.g.,* hurricanes, windstorms, earthquakes, intentional cyber attacks, terrorist attacks. Modern energy systems are increasingly exposed to the threat of extreme events, causing enormous damages to business, economy and society [1]. For example, a survey by the U.S. energy information administration observed an significant increase of power outages caused by extreme weather events from 1992 to 2002 [2]. In 2008, 14.66 million households were affected by power outages caused by a snow storm in southern China [3]. The east Japan earthquake in 2011 made four million households suffering from power outage for seven to nine days [3]. Worse still, the occurrence rates of accidents caused by extreme events are expected to keep increasing, for reasons like climate changes and aging of energy infrastructures.

Resilience is generally acknowledged as the ability of a system to resist, mitigate and quickly recover from potential disruptions [4]. Faced with the increasing threat from extreme events, resilience has become an indispensable requirement on modern energy systems. Hence, a large number of researches on resilience modelling and analyses have been conducted (a detailed literature review is presented in Sect. II). Most existing works, however, apply only for systems whose performance can be quantified by a continuous variable. In practice, however, a lot of energy systems are multistate in nature, or can only be modeled using multistate models to control the complexity of modelling. For example, in , the performance of a oil storage tank farm is modeled by a discrete multistate model. Demands, capacities and performances of energy systems are often described by multistate models [5]. How to quantify the resilience of such multistate systems, then, remains an open research issue.

Markov processes are powerful tools for describing multistate behaviors of energy systems. Rahnamay-Naeini et. al. *[6] developed a continuous-time Markov model as a scalable and analytically tractable tool for analyzing cascading failure dynamics in power grids. A discrete Markov power system model was developed in [7] and used to investigate the angle stability of the power grid considering multiple operation conditions and possible cascading failures. Sanghavi* et. al. *[8] used Markov processes to model cascading failures in a large-scale cloud computing infrastructure and assessed its dependability. In [9], a Markov model was used for searching cascading failure paths in a power grid considering high wind power penetration. However, Markov*

models cannot be directly applied for modelling system resilience, as the latter requires not only capturing system behaviors, but also the losses incurred by performance degradation. Markov Reward Process (MRP) is a Markov model with reward structures, where reward rates are defined associated with sojourns in the states or state transitions in the Markov model [10]. This provides a natural way to describe the dynamics of system performance and losses prior to and after the disruptive event, making MRP an ideal tool for modelling resilience of multistate systems. In this paper, we develop a MRP-based model for resilience modelling and analysis of multistate energy systems. Compared to the existing works, the contributions of this paper include:

- a resilience model is developed for multistate systems based on Markov reward processes;
- four resilience metrics are defined to measure different aspects of resilience;
- a simulation-based algorithm is developed for resilience analysis of multistate systems.

The rest of the paper is organized as follow. Sect. II presents a state-of-art review of related works. In Sect. III, we present the developed resilience model, numerical metrics and the simulation-based algorithm for resilience analysis. In Sect. IV, the developed methods are applied in a real world case study of a Nuclear Power Plant (NPP). Finally, the paper is concluded in Sect. V with a discussion of potential future works.

II. Literature review

A. Resilience: Concepts and definitions

The word "resilience" is originated from the Latin word "resiliere", which means "to bounce back" [4]. Although its original meaning only focuses on the capability of recovering to normal states, the concept of resilience has been greatly generalized, through applications in different domains, to cover other important aspects like the ability to resist and absorb the damages caused by disruptive events. For example, resilience is defined by the American Society of Mechanical Engineers (ASME) as "the ability of a system to sustain external and internal disruptions without discontinuity of performing the system's function or, if the function is disconnected, to fully recover the function rapidly" [4]. National Infrastructure Advisory Council (NIAC) defined the resilience of infrastructure systems as "their ability to predict, absorb, adapt, and/or quickly recover from a disruptive event such as natural disasters" [11].

A large number of resilience definitions can be found in literature. Different definitions, however, concentrate on different aspects of resilience. For example, Holling [12] defined resilience as "the persistence of systems and of their ability to absorb change and disturbance and still maintain the same relationships between populations or state variables." By doing so, his definition concerns the ability of a system to resist and absorb the potential damages of a disruptive event, while do not consider the recovery capability. Similar definitions have been adopted by many researchers. For instance, resilience was defined by Pregenzer [13] as the "a system's ability to absorb continuous and unpredictable change and still maintain its vital functions." Allenby and Fink [14] defined resilience as the "capability of a system to maintain its functions and structure in the face of internal and external change and to degrade gracefully when it must." Hollnagel et al. [15] presented a similar definition of

engineering resilience: "the intrinsic ability of a system to adjust its functionality in the presence of a disturbance and unpredicted changes."

Other researchers, on the other hand, view resilience as recovery capability only, and do not consider the resistant and absorption capability. For example, Sheffi [16] defined resilience of companies as "the company's ability to, and speed at which they can, return to their normal performance level following disruptive events." Pfefferbaum et al. [17] defined community resilience as "the ability of community members to take meaningful, deliberate, collective action to remedy the effect of a problem, including the ability to interpret the environment, intervene, and move on." Iervolino and Giorgio [18] defined the seismic resilience as the characteristic of an system which "measures its capability to rapidly recover from a shock."

Most researchers, however, adopt a holistic view on resilience that integrate the resistant, absorption and recovery capabilities together. For example, resilience is defined in [19] as the "ability of system to withstand a major disruption within acceptable degradation parameters and to recover with a suitable time and reasonable costs and risks." Disaster resilience is characterized by Infrastructure Security Partnership [20] as "the capability to prevent or protect against significant multi-hazard threats and incidents, including terrorist attacks, and to recover and reconstitute critical services with minimum devastation to public safety and health." Vugrin *et al.* [21] defined system resilience as: "given the occurrence of a particular disruptive event (or set of events), the resilience of a system to that event (or events) is that system's ability to reduce efficiently both the magnitude and duration of deviation from targeted system performance levels." The resilience of an organization is defined by Sheffi [22] as "the inherent ability to keep or recover a steady state, thereby allowing it to continue normal operations after a disruptive event or in the presence of continuous stress." Resilience is defined in [23] as a result of a system (i) preventing adverse consequences, (ii) minimizing adverse consequences, and (iii) recovering quickly from adverse consequences.

To conclude, it can be seen from above discussions that a complete description of resilience should cover the following aspects:

- resistant capability, *i.e.,* the capability to resist the impact of the disruptive event and remain normal operations;
- absorption capability, *i.e.,* the capability to absorb the influence of the disruptive event (possibly by degrading its performance) and still remains resilient, so that the system can return to normal operation states when the disruptive event disappears;
- recovery capability, *i.e.,* the capability to quickly restore normal operation after the disruptive event disappears.

Most of the current works on resilience focus on only some of these aspects. A unified and comprehensive framework for resilience quantification, which is able to consider all the aspects mentioned above, both separately and collectively, is lacking. In this paper, we develop a comprehensive resilience modelling and analysis framework that covers the three aspects, both separately and collectively.

B. Resilience modelling and analysis of energy systems against extreme events

There are a number of works dedicating to quantifying resilience of energy systems, and, more broadly, engineering systems, against extreme events [1]. Hosseini *et al.* [4] classifies these efforts into two categories: the general measure-based methods and the structure-based methods. In the general measure-based methods, resilience is quantified based on empirically observable quantities, while the system-specific characteristics like system structures are not considered. The structure-based methods, on the contrary, develop resilience models by considering the system-specific characteristics [4].

1) General measure-based methods: A typical example of the general measure-based methods is the resilience triangle model proposed by Bruneau *et al.* [24] for quantifying resilience against seismic risks. In this model, resilience is quantified based on the performance loses (which is empirically observable) induced by the earthquake and during the recovery process. The resilience triangle model has been adopted and extended by many researchers and applied in various domains [25]. In particular, Zobel and Khansa [26] extended the resilience triangle model to consider the resilience against multiple extreme events by assuming a linear recovery process. Panteli *et al.* [27] considered the situation in power system resilience analysis where a delay time is needed before recovery process starts. The resilience triangle is extended to resilience trapezoid. Henry and Ramirez-Marquez [28] proposed a resilience model by comparing the recovered system performance to the reduction of performance from the normal state after the disruption. Amirioun *et al.* [29] developed a model that integrates the effect of restoration actions, system reinforcement and event severity to quantify the resilience of micro grid against windstorms. The approaches reviewed so far are deterministic in nature and do not consider the uncertain or stochastic factors that may influence the resilience [4]. To considered these uncertain factors, probabilistic approaches are developed. For example, Chang and Shinozuka [30] introduced a probabilistic approach to measure the resilience following an earthquake, in which the resilience is quantifies by the probability that either damage or recovery time exceeds acceptable thresholds. Ouyang *et al.* [31] proposed a probabilistic extension of the resilience triangle and used it to quantify resilience under multiple extreme events.

2) Structure-based methods: Typical structure-based methods include, according to [4] and [32], optimization-based methods, topology-based methods and simulation-based methods. In optimization-based methods, resilience is evaluated by solving an optimization model that aims to restore the system within the required time while minimizing the potential losses [32]. For example, Alderson *et al.* [33] quantified the resilience of critical infrastructures by using a mixed integer non-linear programming model to find out the best defense strategies that minimizes the total cost. A bi-level optimization model is proposed by Manshadi and Khodayar [34] for resilience analysis of interconnected natural gas and electricity infrastructures. Chen et al. [35] considered the resilience of power networks after major faults caused by natural disasters by developing a mixed-integer linear programming model that maximizes the total prioritized loads restored while satisfying self-adequacy and operation constraints of each microgrid. Yuan et al. [36] considered resilience planning for distribution

system with hardening and distributed generators by developing a two-stage optimization model. Fang et al. [37] developed a combinational multi-objective optimization model to maximize the resilience of electricity transmission systems against cascading failure and minimize investment costs.

In topology-based methods, the resilience is modelled and analyzed based on topological model of the systems (usually in terms of network models). This type of model is often used in vulnerability analyses, which is related to the resistant capability in the definition of resilience. For example, Page *et al.* [38] proposed a topological model-based framework for modelling, simulating and optimizing the vulnerability and resilience of energy networks. Chen *et al.* [39] proposed a hybrid model for vulnerability (resilience) analysis that combines topological models with important characteristics of the power transmission networks like power flow distributions. In Liu *et al.* [40], the topological model was combined with system dynamic models for resilience quantification of interconnected gas and electricity networks.

In simulation-based methods, simulation methods like Monte Carlo simulations are used to capture the uncertain behaviors involved in the resilience quantifications. For example, in [41], a time-series simulation model based on Monte Carlo methods is developed to evaluate the resilience of power system under the impact of extreme whether events. Cardini *et al.* [42] developed a simulation model that is able to consider the system behavior under both normal and extreme whether events for resilience quantification. Li *et al.* [43] applied the simulation-based method to investigate the resilience of power distribution systems against hurricanes. Rocchetta *et al.* [44] proposed a simulation-based framework to evaluate the resilience of power grids subject to extreme weather-induced failures.

Most of the existing resilience modelling and analysis approaches, as reviewed above, are designed for systems with a continuous performance levels. In practice, however, a lot of energy systems are modelled as multistate systems, where the system performance takes only discrete values [45]. How to quantify the resilience of these multistate system remains an open issue. Hence, we develop a MRP-based model which allows a comprehensive resilience assessment of multistate energy systems in this paper.

III. The developed resilience model

In this section, we present the developed MRP-based resilience model in Sect. III-A. Then, four numerical metrics are defined in Sect. III-B for measuring resilience. In Sect. III-C, we discuss how to use the developed model for resilience analysis and present a simulation-based method for evaluating the defined resilience metrics.

A. A Markov reward process model for resilience

Let $X(t), t > 0$ represents the performance of a system at t under the threat of possible disruptive events. Without losing generality, let us assume that $X(t)$ takes $(m+1)$ discrete values: $X(t) \in [0, 1, 2, \cdots, m]$, where 0 represents the highest performance (perfect state) while m represents the lowest one, and that $X(t)$ is a continuous time discrete state Markov with a transition rate matrix Q (also called intensity matrix or

infinitestimal generator matrix in some literature):

$$Q = \begin{bmatrix} q_{00} & q_{01} & \cdots & q_{0m} \\ q_{10} & q_{11} & \cdots & q_{1m} \\ \vdots & \vdots & \ddots & \vdots \\ q_{m0} & q_{m1} & \cdots & q_{mm} \end{bmatrix}$$

where $q_{i,j}, 0 \leq i,j \leq m, i \neq j$ are the rates that the system departs from state i and ends in state j and $q_{i,i} = -\sum_{j \neq i} q_{i,j},, 0 \leq i \leq m$. At $t = 0$, it is assumed that the system is in the perfect state ($X(0) = 0$). The jumps that degrade the system's performance (from state i to state j where $i < j$) are results of damages caused by disruptive events, while the jumps that improve the performance represent recovery of the system.

Typically, disruptive events can incur two types of losses on the system: the direct losses, which are generated directly by the disruptive event and do not depend on the length of the disruption; and the indirect losses, which are caused by the degraded system performances and depend on the length of the recovery process (*e.g.,* downtime costs) [46]. Take an NPP as an example. When an earthquake occurs, damages might be caused to the NPP as a direct result of the earthquake shake (*e.g.,* structural damages to the NPP, failure of components). The losses associated with these damages are called direct losses. After the earthquake, the NPP might be shut down for repairs. Financial losses are also incurred during this shutdown period due to the lost potential revenues. This kind of losses is an example of indirect losses.

To model the losses caused by the extreme events, we introduce the MRP model in Figure 1: the system suffers a direct loss of $d_{i,j}$ when it jumps from state i to state j due to the disruptive event, where

$$\begin{cases} d_{i,j} > 0, \text{ if } i < j, \\ d_{i,j} = 0, \text{ if } i \geq j. \end{cases} \tag{1}$$

Besides, the system also suffers an indirect loss of l_i (per unit of time) for its sojourn in the performance degradation state $i, 1 \leq i \leq m$.

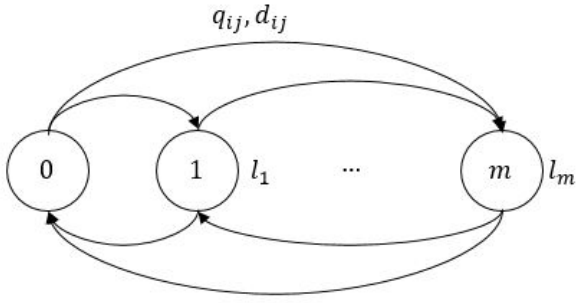

Fig. 1: Markov reward model for resilience against extreme events.

B. Resilience metrics

As shown in Sect. II-A, resilience of a system includes requirements on the resistant, absorption and recovery capabilities. In the following, we propose formal definitions and numerical metrics for the three aspects of resilience individually, and then propose a collective numerical metric to quantify the overall resilience of the system of interest.

Definition 1 (Resistant resilience)**.** *Resistant resilience is the ability of a system to resist the influence of extreme events without degrading its performance.*

As shown in Definition 1, resistant resilience requires the system to remain operational without performance degradations after being hit by the extreme event. In other words, a system with high resistant resilience is able to operate at full capacity after the extreme event, without the need of being repaired. Resistant resilience is often achieved through strengthening system designs, *e.g.,* strengthening structure strengths, selecting highly reliable components.

Based on the MRP model in Sect. III-A, we define a numerical metric, called resistant probability (p_{Rs}), to measure the resistant resilience of a system at time t.

Definition 2 (Resistant probability)**.** *Resistant probability at time t is defined as the probability that the system can be operated at perfect performance in $(0, t)$.*

From Definition 2, p_{RS} can be calculated by

$$p_{Rs}(t) = Pr\left(X(\tau) = X_0,\ \forall \tau \in (0, t)\right), \tag{2}$$

where X_0 is the state with perfect system performance level. The physical meaning of p_{Rs} is the probability that the system is able to resist the impact of the extreme event. It is easy to see that p_{Rs} takes values in $[0, 1]$ and that a larger value of p_{Rs} indicates better resistant resilience. It should be noted that if we regard the event $X(t) \neq X_0$ as system failure, resilient probability is equivalent to the reliability of the system (probability of no system failure up to time t), which, according to some researchers, is an important contributor to system resilience [47].

Definition 3 (Absorption resilience)**.** *Absorption resilience is the capacity of a system to absorb the impact of extreme events so that it can be recovered to normal operation state after the extreme event vanishes, without causing permanent damages to the system.*

Absorption resilience is less demanding compared to the resistant resilience. Performance degradation is allowed as long as the impact of the extreme events can be absorbed so that the system remains in resilient states. Resilient states represent the states without permanent damages, so that the system is recoverable after the extreme events disappear. In contract, in some states, the system loses resilience. For example, an NPP

attacked by an earthquake loses its resilience if the safety systems fail to promptly shutdown the NPP and a core meltdown accident occurs, like what happens in the Fukushima or Chernobyl accident. In both cases, the system loses resilience as the NPPs have to be abandoned and cannot be repaired.

To measure the absorption resilience, let us first group the state space of $X(t)$ into two classes: B_0, which contains all the resilient states, and B_1, which includes all states in which the system loses its resilience (core meltdown accidents in NPPs, complete broken down of dams by flooding, *etc.*). Then, a numerical metric, called resilient probability (p_{Re}), can be defined to measure the absorption resilience:

Definition 4 (Resilient probability)**.** *Resilient probability at time t is defined as the conditional probability that the system remains resilient up to time t, given that disruptions occurred before t:*

$$p_{Re}(t) = Pr\left(X(t) \in B_0 \mid X(\tau) > 0, \exists \tau \in (0,t)\right). \tag{3}$$

It should be noted that as the non-resilient states are unrecoverable, we only need to require that $X(t) \in B_0$, rather than $X(\tau) \in B_0, \forall \tau \in (0,t)$. The physical meaning of p_{Re} is the probability that the system is able to absorb the impact of the extreme event (possibly with performance degradation) without losing resilience. It is easy to see that p_{Re} takes values in $[0,1]$ and that a larger value of p_{Re} indicates better absorption resilience. It should be noted that if we regard the states in B_1 as an undesired consequence in conventional risk analyses, p_{Re} is equivalent to the non-occurrence probability of such consequence. In engineering practice, safety barriers are often designed to prevent the system from entering the loss-of-resilience states. For example, in NPPs, a number of safety barriers (high pressure coolant injection system, automatic depressurization system, low pressure coolant injection system, *etc.*) are used in a defence-in-depth architecture to prevent severe consequences like core meltdown from happening. Adding safety barriers like these can help reduce p_{Re} and improve the absorption resilience.

Definition 5 (Recovery resilience)**.** *Recovery resilience is the capacity of a system to recover to normal operation state within required time limits after its performance is disrupted by the extreme event.*

As shown in Definition 5, recovery resilience is about whether a system can be repaired promptly within a prescribed time limit. In practice, recovery resilience depends largely on the distribution of the time needed to recover the system, which further depends on factors like maintenance resources prepared for the system, training of the maintenance personnel, *etc*. A numerical metric, called recovery probability (p_{Rc}), is defined to measure the recovery resilience:

Definition 6 (Recovery probability)**.** *Recovery probability at time t is defined as the conditional probability that the system operated in $(0,t)$ is recovered to normal operation state within a prescribed time limit $T_{th,Rc}$, given that its performance is disrupted by an extreme event.*

Let us define a random variable $T_i(t)$ to represent the accumulated sojourn time at state $i, i = 0, 1, \cdots, m$ in $(0, t)$:

$$T_i(t) = \int_0^t \mathbb{1}\{X(u) = i\}\, \mathrm{d}u, \tag{4}$$

where $\mathbb{1}\{X(u) = i\}$ is an indicator function:

$$\mathbb{1}\{X(u) = i\} = \begin{cases} 1, \text{ if } X(u) = i, \\ 0, \text{ otherwise.} \end{cases} \tag{5}$$

Then, p_{Rc} can be calculated by:

$$p_{Rc}(t) = Pr\left(T_{Rc}(t) \leq T_{th,Rc} \mid X(\tau) > 0, \exists \tau \in (0, t)\right). \tag{6}$$

where $T_{th,Rc}$ is the prescribed time threshold for system recovery; $T_{Rc}(t)$ is the accumulated recovery time in $(0, t)$ and is given by

$$T_{Rc}(t) = \sum_{i>0} T_i(t). \tag{7}$$

The physical meaning of p_{Rc} is the probability that the system is able to recover to normal operation states within required time limits. It is easy to see that p_{Re} takes values in $[0, 1]$ and that a large value of p_{Rc} indicates better recovery resilience. Similar metrics have been seen in literature to measure the resilience from a recovery capability-based perspective. For example, in [48], resilience is measured by the conditional probability that a failed item will be recovered in the next time step, which is equivalent to Eq. (6) if we considered $T_{th,Rc}$ to be "the next time step".

Definition 7 (Overall resilience)**.** *Overall resilience is the capacity of a system to sustain external and internal disruptions without degrading its performance or, if the performance is degraded, to fully recover the function rapidly after the disruption vanishes.*

Overall resilience integrates the resistant, absorption and recovery resilience and provides a more complete description of system resilience. Similar definitions can also be found in literature (*e.g.,* [19], [21] and [22]). To quantitatively measure the overall resilience, let us first note that the resistant, absorption and recovery resilience can be naturally integrated through the potential losses suffered by the system:

$$\begin{aligned} L(t) &= L_D(t) + L_{ID}(t) \\ &= \sum_{i=0}^{m} \sum_{j=0}^{m} d_{i,j} \cdot N_{i,j}(t) + \sum_{i=0}^{m} l_i \cdot T_i(t), \end{aligned} \tag{8}$$

where $L_D(t), L_{ID}(t)$ and $L(t)$ are the direct, indirect and total loss in $(0, t)$, respectively; $N_{i,j}(t)$ is the number of system transitions from state i to j in in $(0, t)$; $d_{i,j}$ and l_i are defined in Figure 1 while $T_i(t)$ is defined

in Eq. (4). In the above definition, the resistant and absorption resilience affect the direct losses, while the recovery resilience mostly affects the indirect loss. Assume that a resilience objective is set in such a way that the potential loss for the system operating in $[0, t]$ should not exceed a prescribed value of L_{tol}. Then, a numerical metric for the overall resilience, called overall resilience metric (Re), can be defined.

Definition 8 (Overall resilience metric)**.** *Overall resilience metric at time t is defined as the probability that the potential losses caused by extreme events are within the tolerable loss L_{tol}:*

$$Re(t) = Pr(L(t) < L_{tol}). \tag{9}$$

The physical meaning of Re is the probability that the system does not suffer financial losses higher than a predefined threshold value L_{tol}. It is easy to see that Re takes values in $[0, 1]$ and that a larger value of Re indicates better overall resilience. The idea of using losses to quantify resilience has been adopted by various researchers. For example, it is easy to verify from Figure 2 that if we set $d_{i,j} = 0$ and $l_i = m - i, i, j = 0, 1, \cdots, m$, the total loss in Eq. (8) (the shaded area in Figure 2) is equivalent to the resilience triangle defined in [24]. The expected value of $L(t)$ has been widely used as a reliability metric [49], and also as a resilience metric recently [44], for electrical power system. Similar metrics are found in areas similar to resilience, *e.g.,* business continuity modelling [46], performability analysis [50]. In this paper, we also call Re overall resilience for simplicity if no confusion will be caused.

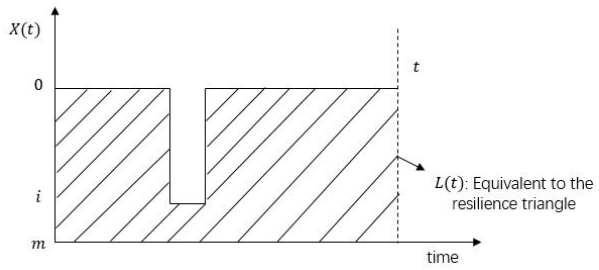

Fig. 2: A sample trajectory of $X(t)$ and $L(t)$ with $d_{i,j} = 0$ and $l_i = m - i$.

C. Resilience modelling and analysis against the extreme events

Figure 3 depicts a typical event sequence after the system is hit by an extreme event. In the response phase, the built-in safety systems are activated to contain the damage caused by the extreme event. Depending on the performance of the safety systems, different consequences with different degree of damages can be resulted. After the extreme event vanishes, efforts are made to recover the system to normal operation state. Depending on the severity of consequence and also on the maintainability of the system, the required time to recovery might differ significantly.

Homogeneous Poisson processes are widely used in literature for modelling extreme events such as earthquakes [51], floods [52], hurricanes [53], etc. In this paper, we assume that the severity of the extreme event

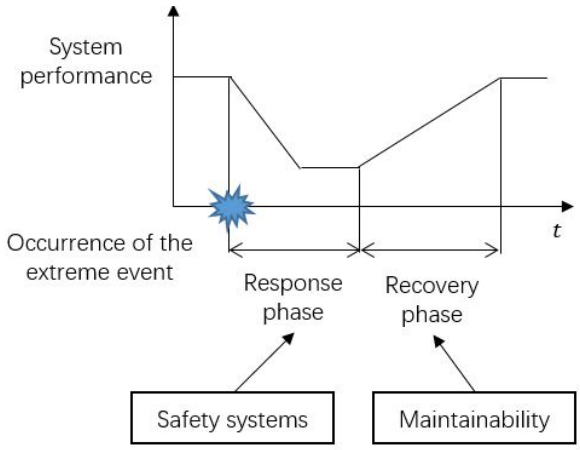

Fig. 3: An illustration of the event sequence after the extreme event.

can be classified into n_S discrete levels, and the occurrence of an extreme event with severity level $S = S_i$ is modelled by a homogeneous Poisson process with a rate $\lambda_{S,i}, i = 1, 2, \cdots, n_S$. The values of $\lambda_{S,i}$ can be estimated from historical data. For example, [54] proposed a method to estimate the discretized values of $\lambda_{S,i}$ for earthquakes based on historical data and an empirical relationship called Gutenberg-Richter relationship.

Once the extreme event occurs, the system's performance might degrade, depending on the performance of the safety systems. Probabilistic combinational models, such as event trees, fault trees, binary decision diagrams, etc. [55], can be used to describe the performance of the safety systems and calculate the conditional probability for the system to be in each performance degradation state, given that an extreme event with a certain severity occurs, as shown in Figure 4. It is well known that the split and merge of Poisson processes are also Poisson processes [56]. Therefore, the occurrence of each system state $X = i, i = 0, 1, \cdots, m$ can be modelled by a homogeneous Poisson process with a rate λ_i, which is given by

$$\lambda_i = \sum_{j=1}^{n_S} \lambda_{S,j} \cdot Pr\left(X = i \mid S = j\right), 0 \leq i \leq m. \tag{10}$$

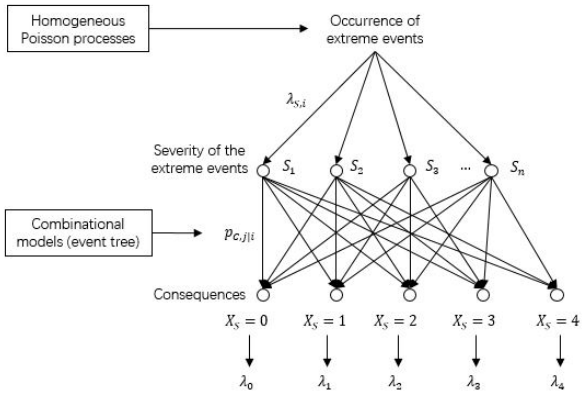

Fig. 4: System states after the disruptive events.

Algorithm 1: Resilience analysis based on Markov reward model

input : $Q, d_{i,j}, l_i$
output: $p_{Rs}(t)$, $p_{Re}(t)$, $p_{Rc}(t)$, $Re(t)$
$n_{Rs} = 0$, $n_{Ab} = 0$, $n_{Rc} = 0$, $n_{Re} = 0$;
for $i \leftarrow 1$ **to** N_S **do**
  Set x_{prev}, x_{cur}, τ, τ_{next}, L_D, L_{ID}, t_{Rc} to zeros;
  while $\tau < t$ **do**
    if $x_{cur} \neq m$ **then** $L_D, L_{ID}, t_{Rc} \leftarrow$ `FnUpdateStates`;
    else break;
    $x_{prev} \leftarrow x_{cur}$;
    $x_{cur}, \tau_{next} \leftarrow$ Simulate the next jump of the Markov model using `FnNextJump`;
    $\tau \leftarrow \tau + \tau_{next}$;
  end
  if $\tau == \tau_{next}$ **then** $n_{Rs} = n_{Rs} + 1$;
  if $x_{cur} \neq m$ **then** $n_{Ab} = n_{Ab} + 1$;
  if $t_{Rc} < T_{th,Rc}$ && $t_{Rc} > 0$ **then** $n_{Rc} = n_{Rc} + 1$;
  if $L_D + L_{ID} < L_{tol}$ **then** $n_{Re} = n_{Re} + 1$;
end
$p_{Rs}(t) \leftarrow n_{Rs}/N_S$, $p_{Re}(t) \leftarrow n_{Ab}/(N_S - n_{Rs})$, $p_{Rc}(t) \leftarrow n_{Rc}/(N_S - n_{Rs})$, $Re(t) \leftarrow n_{Re}/N_S$;
Calculate the confidence intervals.
Function `FnNextJump` (x_{prev}, Q)
  output: x_{cur}, τ_{next}
  $\lambda \leftarrow -1 \cdot Q(x_{prev}, x_{prev})$;
  $\tau_{next} \leftarrow$ Generate a random number from $Exponential(\lambda)$;
  $p_i \leftarrow Q(x_{prev}, i)/\lambda$, $i = 0, 1, \cdots, m, i \neq x_{prev}$;
  $x_{cur} \leftarrow$ Generate a random number where $x_{cur} = i$ with a probability p_i;
end
Function `FnUpdateStates` $(x_{prev}, x_{cur}, \tau_{next}, d_{i,j}, l_i, L_D, L_{ID}, t_{Rc})$
  output: L_D, L_{ID}, t_{Rc}
  if $x_{prev} < x_{cur}$ **then** $L_D = L_D + d_{x_{prev}, x_{cur}}$;
  if $x_{prev} > x_{cur}$ **then** $L_{ID} = L_{ID} + l_{x_{prev}} \cdot \tau_{next}$;
  if $x_{prev} \neq 0$ **then** $t_{Rc} = t_{Rc} + \tau_{next}$;
end

Without losing generality, we make the following assumptions:

1) states $X = 0, 1, \cdots, m-1$ are resilient states while state $X = m$ is a non-resilient state (absorbing state), *i.e.,* the system cannot be recovered if entering this state;
2) the time required to recover from state i to state j ($i > j$) follows an exponential distribution with a rate $\mu_{i,j}$;
3) there are no damages caused by extreme events during the recovery processes.

Then, a MRP model defined in Sect. III-A can be established with the Q-matrix given by:

$$Q = \begin{bmatrix} -\sum_{i=1}^{m} \lambda_i & \lambda_1 & \lambda_2 & \lambda_3 & \lambda_4 & \dots & \lambda_m \\ \mu_{10} & -\mu_{10} & 0 & 0 & 0 & \dots & 0 \\ \mu_{20} & \mu_{21} & -\sum_{j=0}^{1} \mu_{2,j} & 0 & 0 & \dots & 0 \\ \vdots & \vdots & \ddots & \vdots & \vdots & \ddots & \vdots \\ \mu_{i0} & \mu_{i1} & \dots & -\sum_{j=0}^{i-1} \mu_{i,j} & 0 & \dots & 0 \\ 0 & 0 & 0 & 0 & 0 & \dots & 0 \end{bmatrix}. \tag{11}$$

The zeros in the last row indicates that the state $X = m$ is an absorbing state. The direct ($d_{i,j}$) and indirect losses (l_i) associated with the system states can, then, be determined from historical data.

A simulation method is, then, designed to calculate the resilience metrics, as shown in Algorithm 1. In Algorithm 1, N_S is the sample size of the simulation and $X = m$ indicates the state where the system loses resilience. The meaning of the other parameters can be found in the nomenclature. The algorithm used uniformization techniques [57] to generate the next state jumps. As shown in subfunction FnNextJump, the arrival time for the next jump is generated based on the largest element in each row of Q, while the next state is sampled with a probability proportional to the associated elements in Q. Once the sample paths are generated, the resilience metrics can be easily calculated by counting the direct and indirect losses. The confidence interval with a confidence level α is estimated by [56]:

$$\left[\hat{p} - Z_{1-\alpha/2} \cdot \hat{\sigma}, \hat{p} + Z_{1-\alpha/2} \cdot \hat{\sigma}\right],$$

where $\hat{p}$ is the estimated probabilities (p_{Rs}, p_{Re}, p_{Rc} and Re), Z_θ is the θ percentile of a standard normal distribution and $\hat{\sigma}$ is estimated by:

$$\hat{\sigma} = \sqrt{\frac{1}{N(N-1)}\left(n(1-\hat{p}^2) - (N_S - n)\hat{p}^2\right)},$$

where n is the number of occurrence of the associated event and N_S is the sample size.

IV. Application

In this section, we apply the developed methods for resilience analysis of a nuclear power plant under the threat of earthquakes. The NPP under investigation is briefly introduction in Sect. IV-A. A Probabilistic Seismic Hazard Analysis (PSHA) is, then, conducted in Sect. IV-B to model the occurrence likelihood and magnitude of the earthquake. In Sect. IV-C, a fragility analysis is made to calculate the failure probability of the subsystems of the NPP caused by the earthquake. In Sect. IV-D, event tree analyses are combined with fault tree analyses to calculate the occurrence probabilities of each possible consequence. A MRP model is developed in Sect. IV-E for resilience modelling and analysis. The results and some discussions are presented in Sect. IV-F.

A. System description

In this case study, we consider an NPP with a total power generation capacity of 1898 (MW). The NPP comprises of two units: unit 1 has a power generation capacity of 540 (MW) and unit 2 has power generation capacity of 1358 (MW). The configuration of the NPP is set based on the Shika NPP described in [58]. For simplicity, let us assume that both units could be in one of the three states after the earthquake:

- fully functional ($X_i = 0$), in which the unit is unaffected by the earthquake and can continue normal operation at its full capacity;

- shutdown ($X_i = 1$), in which critical functions of the unit are damaged but the unit is promptly shut down by the safety systems;
- core damage ($X_i = 2$), in which the safety systems fail to promptly shut down the unit. As a consequence, damage is caused to the reactor core and radioactive materials are released to the environment.

In the above definitions, X_i, $i = 1, 2$ represent the state of the first and the second unit, respectively. The severity of the consequence increases from $X_i = 0$ to $X_i = 2$. The severity of the consequences are coherent with the nuclear and radiological event scale defined by IAEA [59]:

- $X_i = 0$ corresponds to IAEA level 0 (deviations, *i.e.,* events without safety significance);
- $X_i = 1$ corresponds to IAEA levels $1 - 3$ (incidents);
- $X_i = 2$ corresponds to IAEA levels $4 - 7$ (accidents).

Depending on the states of the units, the NPP has four possible states (denoted by X_S), with different levels of remaining power generation capacity (Q_S), as shown in Table I.

TABLE I: States of the NPP.

State of the NPP	Meaning	State of the units		Q_S
		X_1	X_2	
$X_S = 4$	Accident with core damages occurs.	$X_1 = 2$ or $X_2 = 2$		\
$X_S = 3$	Both units are shut down for maintenance.	1	1	0 (MW)
$X_S = 2$	Unit 1 is working but unit 2 is shut down for maintenance.	0	1	540 (MW)
$X_S = 1$	Unit 2 is working but unit 1 is shut down for maintenance.	1	0	1358 (MW)
$X_S = 0$	Both units are working.	0	0	1898 (MW)

To maintain the NPP in safe state after earthquake, each unit must be provided with electrical and water inputs to absorb the heat generated by the nuclear reaction. As in [60], we assume that for each unit, two safety systems are available to protect the NPP: internal and external safety systems. As shown in Figure 5, the internal safety system comprises of a pump, a water pool and electricity supply systems. The electricity supplies can be from either an external power generation station or from an emergency diesel generator. Either one of the two power source is sufficient to drive the pump for cooling the reactor core using the cooling water from the water pool. The external safety system uses cooling water from a local river. As the internal safety system, the electricity supplies of the external safety system can be also from the external power generation station or from an emergency diesel generator. The external power station is shared between the internal and external safety systems, while both the internal and the external safety system have its own emergency diesel generator. The external power station is also shared between the two reactor units.

B. Probabilistic seismic hazard analysis

The purpose of PSHA is to estimate the ground motion caused by earthquake that may occur at the NPP, considering all the possible uncertainties. Normally, the ground motion is measured by the Peak Ground Acceleration (PGA) at the site, denoted by A (in units of g). According to [54, 61], PGA depends on

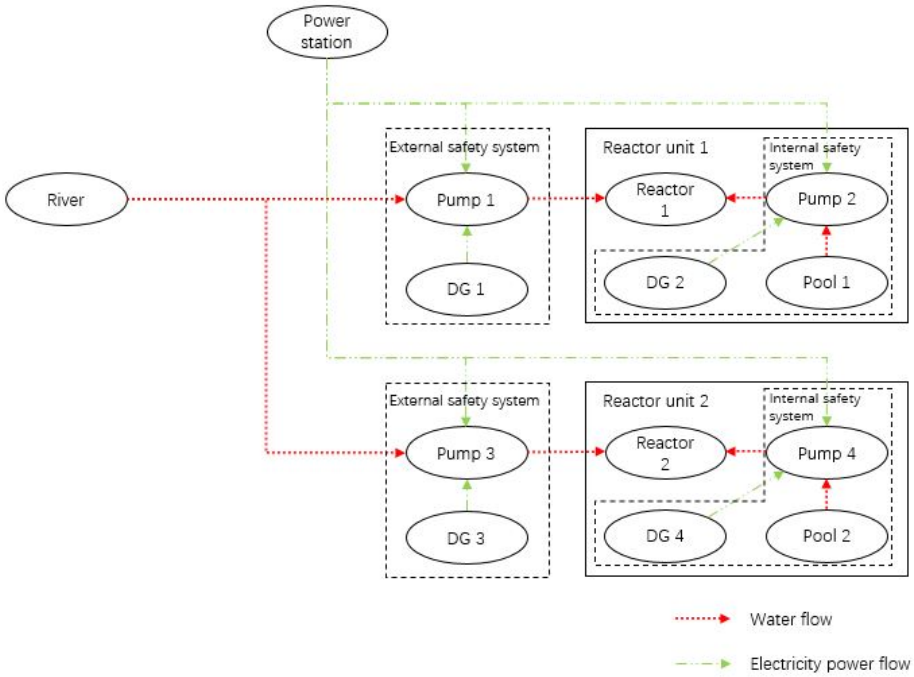

Fig. 5: Illustration of the safety systems of the NPP.

the magnitude of the earthquake (M, in Richter magnitude scale) and the source-to-site distance of the earthquake (D, in kilometers). Cornell *et al.* [62] assumed that the PGA follows Lognormal distribution, *i.e.,* $\ln A \sim Normal(\mu, \sigma^2)$, where $\sigma = 0.57$ and μ (in units of g) is calculated by an empirical equation:

$$\mu = -0.152 + 0.859M - 1.803\ln(D + 25). \tag{12}$$

1) Poisson process model for the earthquake magnitudes: In PSHA, it is often assumed that the occurrence of earthquakes follows a homogeneous Poisson process [51]. The rate for the accumulated number of earthquakes with a magnitude no less than m, denoted by $\lambda_C(M \geq m)$ (in $year^{-1}$), follows Gutenberg-Richter relationship [54]:

$$\log \lambda_C(M \geq m) = a - bm. \tag{13}$$

where a and b are two constants that need to be estimated from historical earthquake data. In this paper, for illustrative purposes, we use the parameter values fitted from the southern California earthquake data between 1903 and 1997: $\hat{a} = 5.9, \hat{b} = 1.0$ [63].

To simplify the analysis, We adopt the approach in [54] to discretize the magnitudes into six discrete levels $m_i, i = 1, 2, \cdots, 6$:

$$\lambda(M = m_i) = \begin{cases} \lambda_C(M \geq m_i) - \lambda_C(M \geq m_{i+1}), \text{if } 1 \leq i < 6. \\ \lambda_C(M \geq m_i), \text{if } i = 6. \end{cases} \tag{14}$$

The calculation is based on the assumption that all the probabilities associated with the magnitudes between

m_i and m_{i+1} are assigned to the discrete value m_i. The results of the discretization are as given in Table II. It should be noted that by making a discretization like this, we only consider the earthquake with magnitudes between 6.5 and 9.0 in our analysis. The earthquakes whose $M < 6.5$ are not considered, as their magnitude is too small to cause any severe damages; the earthquakes with $M > 9.0$ are not considered either, as their occurrence rates are very small.

TABLE II: Discretized magnitude values.

m_i	$\lambda_C(M \geq m_i)$	$\lambda(M = m_i)$
6.5	0.2512	0.1718
7.0	0.0794	0.0543
7.5	0.0251	0.0172
8.0	0.0079	0.0054
8.5	0.0025	0.0017
9.0	0.0008	0.0008

2) Modelling the source-to-site distance: As in [54], we use the area source model to model the the source-to-site distance (denoted by D). This model assumes that earthquakes appear randomly and with equal likelihood anywhere within a circular area with a radius Ra from the site of interest (the NPP), as shown in Figure 6. This model indicates that the earthquake source is truncated at some distance Ra beyond which earthquakes are not expected to cause damage to the NPP. As we used the southern California earthquake data to estimate the parameters of the Gutenberg-Richter model in Eq. (13), Ra is selected based on the area of southern California $(146,347\ (\text{km}^2))$:

$$Ra = \sqrt{\frac{146,347}{\pi}} = 215.83\ (\text{km}). \tag{15}$$

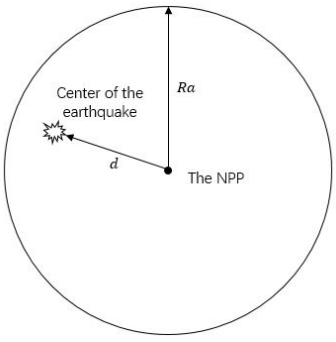

Fig. 6: Illustration of an example area source.

Then, the Probability Density Function (PDF) of D is given by [54]:

$$f_D(d) = \begin{cases} \dfrac{2d}{Ra^2}, & 0 \leq d \leq Ra, \\ 0, & \text{otherwise.} \end{cases} \tag{16}$$

To simplify the analysis, we use the expected value of D to represent the source-to-site distance:

$$E_D = \int_0^{Ra} x f_D(x) dx = \frac{2}{3} Ra = 143.89 \text{ (km)}. \tag{17}$$

The calculated E_D is, then, used in Eq. (12) for evaluating the PGA. Under each magnitude level in Table II, the PGA is a random variable that follows a Lognormal distribution. To simplify the analysis, we use the median of the Lognormal distribution to represent the PGA value under each magnitude level, as shown in Table III.

TABLE III: PGA under each magnitude level.

m_i	6.5	7.0	7.5	8.0	8.5	9.0
a_i (g)	0.0220	0.0338	0.0519	0.0798	0.1226	0.1884

C. Fragility analysis

Table II and III summarize the six typical scenarios considered in this paper with corresponding earthquake magnitudes and the resulted PGA at the NPP. Next, a seismic fragility analysis is carried out to determine the probability of failure of the safety systems caused by the earthquake for each scenario. The fragility model in [45, 61] is used in this paper, where the capacity of a safety system to the impacts of the PGA is assumed to be:

$$A_m \cdot E_a \cdot E_e. \tag{18}$$

In the model, A_m is the best estimate of the capacity and is a constant value; E_a and E_e are two random variables that accounts for the aleatory and epistemic uncertainty on A_m, respectively. Both E_a and E_e are assumed to follow Lognormal distribution with a log mean value of 1. The log standard deviations for E_a and E_e are σ_a and σ_e, respectively. If the PGA at the NPP exceeds the capacity, the corresponding safety system fails. Given a confidence level α, the conditional probability that a safety system is failed by an earthquake with a PGA value a can be calculated by [61]:

$$p_f = \Phi\left(\frac{ln\left(\frac{a}{A_m}\right) + \sigma_e \Phi^{-1}(\alpha)}{\sigma_a}\right). \tag{19}$$

The parameter α is introduced to compensate for the epistemic uncertainty on A_m: we have $100 \cdot \alpha\%$ confidence that the actual probability of failure is less than the calculated p_f by Eq. (19). In this case study, we choose $\alpha = 0.5$.

Let us assume that both units in the NPP share the same design, so that the fragility parameters of the pump, DG and pool are the same for both units. The parameter values from [60] are used for the analysis (see Table IV). The calculated failure probabilities of the safety systems are given in Table V.

TABLE IV: Fragility parameter [60].

	A_m	σ_a	σ_e
Diesel generator	0.7	0.4	0.2
Pool	0.2	0.1	0.1
Power station	0.7	0.3	0.1
Pump	0.2	0.2	0.3

TABLE V: Results of fragility analyses.

Scenarios		Probability of failure			
m_i	a_i (g)	DG ($p_{f,DG}$)	Pool ($p_{f,pool}$)	Power station ($p_{f,PS}$)	Pump ($p_{f,pump}$)
6.5	0.0220	2.5839×10^{-18}	0	0	0
7.0	0.0338	1.7839×10^{-14}	0	0	3.1140×10^{-19}
7.5	0.0519	3.9602×10^{-11}	0	2.1707×10^{-18}	7.8980×10^{-12}
8.0	0.0798	2.8438×10^{-8}	0	2.2800×10^{-13}	2.1857×10^{-6}
8.5	0.1226	6.6654×10^{-6}	5.0218×10^{-7}	3.1965×10^{-9}	7.2348×10^{-3}
9.0	0.1884	5.1747×10^{-4}	0.2757	6.0864×10^{-6}	0.3829

D. Consequences of the earthquake

As shown in Table I, five consequences with different degrees of severity might be caused by the earthquake. Event tree analyses are conducted to calculate the occurrence probability of the consequences, given that an earthquake with magnitude m_i occurs ($i = 1, 2, \cdots 6$). Let us denote the conditional occurrence probabilities by $p_{C,j \mid i}, j = 0, 1, \cdots, 4$, where j corresponds to the state $X_S = j$ in Table I.

For the event $X_S = 4$, an event tree model is constructed in Figure 7, where the Initiating Event (IE) is the occurrence of an earthquake with a given magnitude. From the event tree model, $p_{C,4}$ can be easily calculated as:

$$\begin{aligned} p_{C,4} &= Pr(X_S = 4 \mid \text{The initiating event occurs}) \\ &= p_{f,PS} \cdot Pr(E_1 \mid E_{PS}) + (1 - p_{f,PS}) \cdot Pr(E_1 \mid \bar{E}_{PS}), \end{aligned} \tag{20}$$

where $p_{f,PS}$ is the failure probability of the power station; events E_{PS} and $\bar{E}_{PS}$ represent that the power system fails and does not fail, respectively; event E_1 represents that at least one reactor unit loses all the safety systems.

Fault tree models are further developed to describe the event sequences that lead to E_1, conditioned on the occurrence or non-occurrence of E_{PS}, as shown in Figure 8. Based on the models in Figure 8, $Pr(E_1 \mid E_{PS})$ and $Pr(E_1 \mid \bar{E}_{PS})$ can be easily derived [55]:

$$\begin{aligned} Pr(E_1 \mid E) &= 1 - (1 - Pr(U_1 \mid E))(1 - Pr(U_2 \mid E)) \\ &= 1 - (1 - Pr(U_1 \mid E))^2, \end{aligned} \tag{21}$$

where E takes values in $\{E_{PS}, \bar{E}_{PS}\}$, U_i represents the event "unit i lost all the safety systems" and $Pr(U_1|E))$

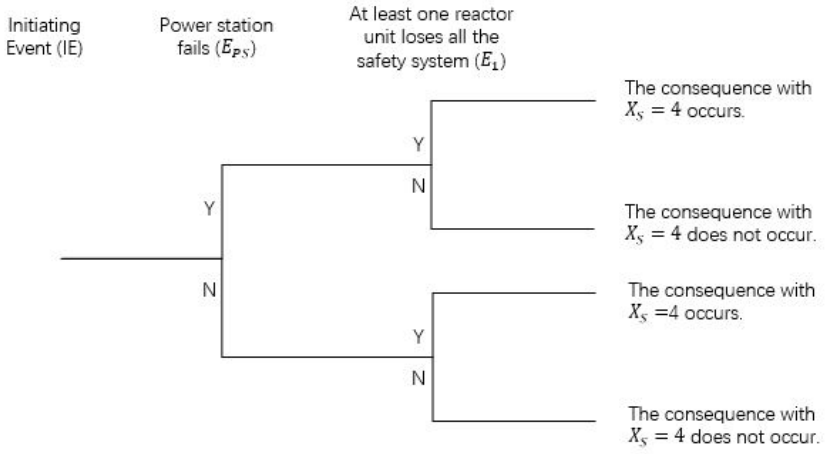

Fig. 7: Event tree model for $X_S = 4$.

is given by:

$$Pr(U_1 \mid E)) = \begin{cases} (1-(1-p_{f,pump})(1-p_{f,DG}))(1-(1-p_{f,pump})(1-p_{f,DG})(1-p_{f,pool})), \text{ if } E = E_{PS}, \\ p_{f,pump}(1-(1-p_{f,pump})(1-p_{f,pool})), \text{ if } E = \bar{E}_{PS}. \end{cases} \tag{22}$$

Substituting the probabilities of failure in Table V into Eqs. (20)-(22), we can calculate the value of $p_{C,4 \mid i}$. Similarly, we can calculate the probability of occurrence of each consequence, under different earthquake magnitudes. The results are summarized in Table VI.

TABLE VI: Probability of occurrence of the consequences.

m_i	$\lambda(M = m_i)$ (year^{-1})	$p_{C,0 \mid i}$	$p_{C,1 \mid i}$	$p_{C,2 \mid i}$	$p_{C,3 \mid i}$	$p_{C,4 \mid i}$
6.5	0.1718	1	0	0	0	0
7.0	0.0543	1	0	0	0	0
7.5	0.0172	1	0	0	0	0
8.0	0.0054	0.9999	4.4283×10^{-6}	4.4283×10^{-6}	1.9838×10^{-11}	9.5548×10^{-12}
8.5	0.0017	0.9712	1.4221×10^{-2}	1.4221×10^{-2}	2.0823×10^{-4}	1.0469×10^{-4}
9.0	0.0008	0.0412	0.1240	0.1240	0.3261	0.3887

As shown in Table VI, the consequences can be caused by earthquakes with different magnitudes, as shown in Figure 9. It is well-known that the aggregation of Poisson processes is also a Poisson process [56]. Therefore, the occurrence of consequence $j, j = 0, 1, \cdots, 4$ can be modeled by a Poisson process with a rate λ_j :

$$\lambda_j = \sum_{i=1}^{6} \lambda(M = m_i) \cdot p_{C,j \mid i} \tag{23}$$

where $p_{C,j \mid i}$ is the occurrence probability for consequence j, given that an earthquake with magnitude $M = m_i$ occurs. The values of $\lambda_j, j = 0, 1, \cdots, 4$ are calculated based on Eq. (23) and the results in Table II and VI, as shown in Table VII.

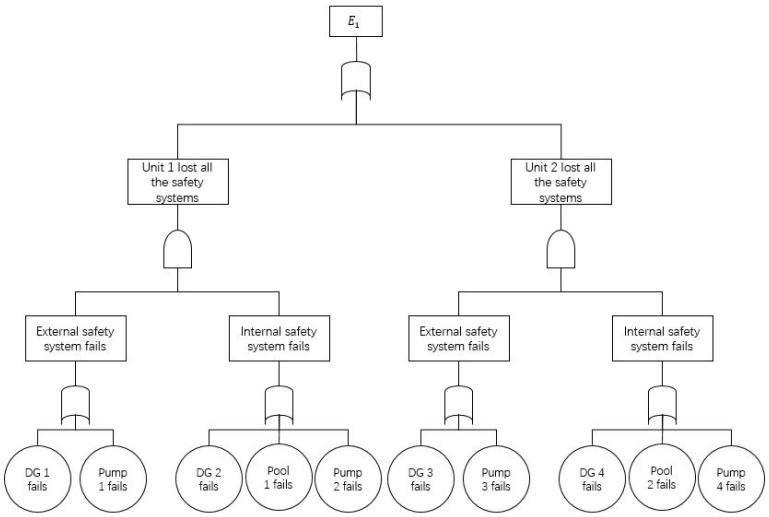

(a) The power station fails.

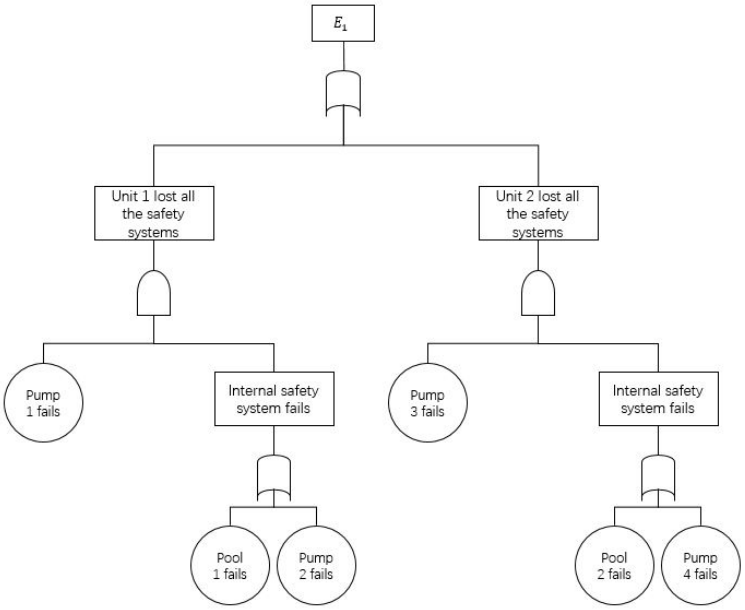

(b) The power station does not fail.

Fig. 8: Fault tree models for E_1.

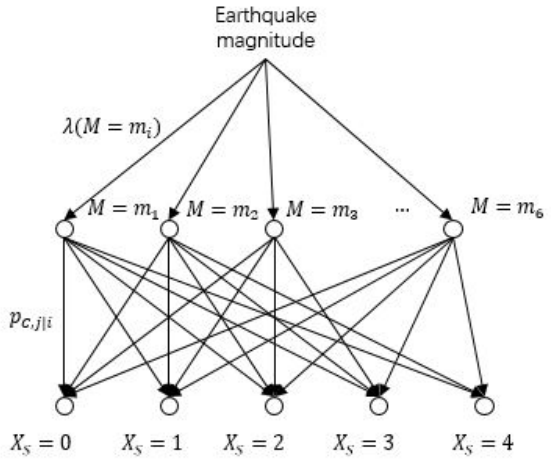

Fig. 9: An illustration of the consequences.

TABLE VII: Rates for the consequences.

Consequence	$X_S = 0$	$X_S = 1$	$X_S = 2$	$X_S = 3$	$X_S = 4$
λ_j (year^{-1})	2.5038×10^{-1}	1.2298×10^{-4}	1.2298×10^{-4}	2.5939×10^{-4}	3.0095×10^{-4}

E. Resilience modelling

To model the recovery process after the earthquake, we make the following assumptions:

1) the repair resource can support repairing only one NPP unit at a time;
2) if the two units both fail, unit 2 is repaired before unit 1;
3) the time required to repair one NPP unit (either 1 or 2) follows an exponential distribution with a mean value of 1.32 (years);
4) no damages are caused by earthquakes during the repair period of the NPP.

The repair sequence defined in Assumption 2 is due to the fact that unit 2 has a larger generation capacity than unit 1. The mean repair time in Assumption 3 is estimated based on data from [58]. It should be noted that the time includes both repair time and the time required for evaluation and re-licensing from the nuclear administrative. Then, the behavior of the NPP under the threat of earthquakes can be modeled by a MRP model, as shown in Figure 10. In Figure 10, the transition rates $\lambda_{0,j} = \lambda_j$ that are given in Table VII; the repair rate $\mu = 1/1.32 = 0.76$ (year^{-1}). The value of the direct losses $d_{0,j}, j = 1, 2, 3$ are estimated based on the replacement cost data of NPPs in [64]. The values of the unit indirect losses $l_i, i = 0, 1, 2, 3$ are estimated based on the average electricity price data for house hold users in Europe area given in [65]. The parameter values are summarized in Table VIII.

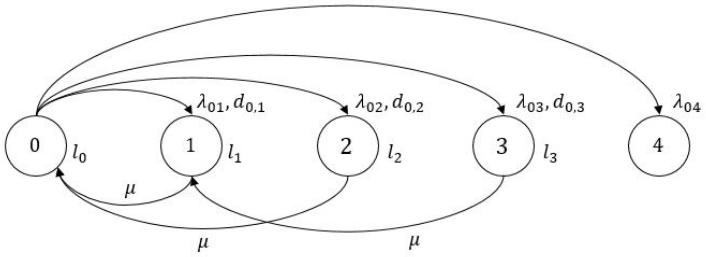

Fig. 10: Markov reward model for the NPP.

TABLE VIII: Parameter values of the Markov reward model.

Parameter	Meaning	Value	Source
$d_{0,1}$	Direct loss caused by the failure of unit 1.	1.8×10^8 (€)	Estimated using the data from [58]
$d_{0,2}$	Direct loss caused by the failure of unit 2.	1.8×10^8 (€)	Estimated using the data from [58]
$d_{0,3}$	Direct loss caused by the failure of unit 1 and 2.	3.6×10^8 (€)	Estimated using the data from [58]
$d_{0,4}$	Direct loss caused by core meltdown.	3.6×10^{10} (€)	Assumed
l_0	Indirect loss (downtime cost) per unit time for staying in state 0.	0 (€)	Estimated using the data from [64]
l_1	Indirect loss (downtime cost) per unit time for staying in state 1.	7.24×10^8 (€/year)	Estimated using the data from [64]
l_2	Indirect loss (downtime cost) per unit time for staying in state 2.	1.82×10^9 (€/year)	Estimated using the data from [64]
l_3	Indirect loss (downtime cost) per unit time for staying in state 3.	2.54×10^9 (€/year)	Estimated using the data from [64]

F. Results and discussions

1) Analyses at a fixed $t = 40$ (years): The Q-matrix of the MRP model in Figure 10 is

$$Q = \begin{bmatrix} -8.0629 \times 10^{-4} & 1.2298 \times 10^{-4} & 1.2298 \times 10^{-4} & 2.5939 \times 10^{-4} & 3.0095 \times 10^{-4} \\ 0.76 & -0.76 & 0 & 0 & 0 \\ 0.76 & 0 & -0.76 & 0 & 0 \\ 0 & 0.76 & 0 & -0.76 & 0 \\ 0 & 0 & 0 & 0 & 0 \end{bmatrix}. \quad (24)$$

Algorithm 1 is used to evaluate the resilience of the NPP for a time horizon of 40 years, which is the designed life of the NPP. The sample size of the analysis is 10^6. The tolerable loss L_{tol} is assumed to be 2.54×10^9 (€) and the acceptable time limit for recovery is assumed to be $T_{Th,Rc} = 2$ (years). The point estimates of the four resilience metrics are presented in Figure 11 and the confidence intervals with confidence level $\alpha = 0.05$ is given in Table IX.

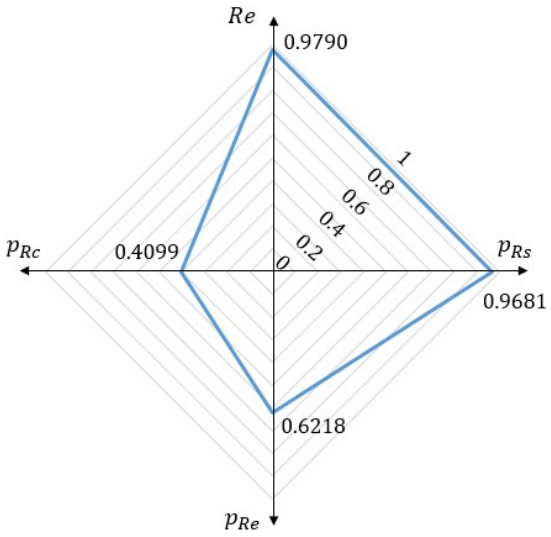

Fig. 11: Results of the resilience analysis ($T = 40$ (years)).

TABLE IX: Confidence intervals with $\alpha = 0.05$.

	p_{Rs}	p_{Re}	p_{Rc}	Re
Lower bound	0.9678	0.6202	0.4045	0.9787
Upper bound	0.9685	0.6233	0.4153	0.9793

It can be seen from Table IX that the confidence intervals are narrow. This indicates that due to the large sample size used (10^6), the estimates are accurate for supporting decision making. The results in Figure 11 describe different aspects of resilience for an NPP being operated up to $t = 40$ (years). For resistant resilience, we have $p_{Rs} = 0.9681$, which indicates that one could have a high degree of belief that the generation capacity

of the NPP will not be disrupted at all by earthquakes in its entire life cycle (40 years). In other words, the probability that NPP keeps operating continuously in the entire evaluation horizon without performance degradation is 0.9681. This is because the design of the NPP and its safety systems is strong for resisting the damages caused by the earthquake. As can be seen in Table V, the failure probabilities of the safety systems remains at a low levels for earthquake magnitudes up to 8.5.

For the absorption resilience, we have $p_{Re} = 0.6218$. This means that if initial disruptions have already occurred, there is only a conditional probability of 0.6218 that the system remains in resilient state in the evaluation horizon, *i.e.,* no core meltdown accidents happen so that the NPP can be repaired after possible performance disruptions caused by the earthquakes. This value might not seem satisfactory, as the core meltdown accident has a very high severity but its probability of occurrence is not low enough. To improve the absorption resilience, two possible approaches might be adopted. The first is to lower the probability of failure of the safety barriers caused by the earthquake by strengthening the anti-seismic designs. The second is to add redundant safety systems to the NPP.

For the recovery resilience, we have $p_{Rc} = 0.4099$, which indicates that there is only a probability of 0.4099 that the recovery time of the NPP can meet its requirements (recovery time should be less than $T_{Th,Rc} = 2$ (years)). This value is far from satisfactory and indicates that the recovery resilience of this NPP needs improvements. A straightforward way to improve the recovery resilience is to reduce the time-to-repair needed under each performance degradation state. There are a number of ways to achieve this, *e.g.,* providing better training to the maintenance personnel, preparing enough resources for the recovery of the NPP. Besides, the measures that improve the resistant and absorption resilience might also improve the recovery resilience. This is because the probability of entering the states with very severe performance degradations (and also requiring very long repair times) can be reduced by improving the resistant and absorption resilience.

For the overall resilience, we have $Re = 0.9790$. This means that there is a probability of 0.9790 that the total losses caused by the earthquake in the evaluation horizon do not exceed $L_{tol} = 2.54 \times 10^9$ (€). As indicated by Re, the NPP demonstrates high overall resilience as the potential losses caused by the earthquake is far below the maximal tolerable losses.

To have a complete picture of the resilience, the four resilience metrics should be considered together. As can be in Figure 11, although the resistant and overall resilience of the NPP are acceptable, its absorption and recovery resilience still need improvement. Hence, efforts are needed to reduce the likelihood that the NPP enters the non-resilient state (core meltdown) and to reduce the needed time to recover the NPP from performance degradation states.

2) Comparison to the $\Phi\Lambda E\Pi$ resilience metrics: In the literature, there are other resilience metrics that also consider the different stages and aspects of resilience. Among them, the $\Phi\Lambda E\Pi$ (pronounced as "FLEP") metrics developed by Panteli et al. *[27] is a most-widely used one. Hence, they are used as a benchmark to compare the strength and limitations of the developed resilience metrics to the existing ones. The definitions of*

the $\Phi\Lambda E\Pi$ metrics are summarized in Table X, highlighting also the specific aspects of resilience each metric describes (detailed information could be found in [27]). Since the $\Phi\Lambda E\Pi$ metrics are defined for individual samples rather than the whole population, five typical realizations (shown in Figure 12) are taken from the Monte Carlo samples generated in the previous section, and used to calculate the $\Phi\Lambda E\Pi$ metrics. The results are given in Table XI. It should be noted that in Sect. IV-A, we assumed that the performance degradation is instantaneous and that the maintenance process starts right after the degradation process finishes. Here, in order to calculate the $\Phi\Lambda E\Pi$ metrics, we replace the first assumption by that the degradation process lasts a random period of time, which follows a Normal distribution with a mean value of 7 days and a standard deviation of 1 day. Also, we assume that the recovery time to a given performance state can be split into two parts: the recovery preparation time, in which the recovery process does not start and the performance remains in the postdisturbance degraded state; and the recovery time, in which repairable operations are carried out to restore the degraded performance. It is assumed that the two parts equally divide the original recovery time in the Monte Carlo samples.

TABLE X: *Definitions of the $\Phi\Lambda E\Pi$ metrics.*

Metric	Definition	Aspect of resilience concerned
Φ	Slopes of performance degradation processes.	Resistant and absorption resilience
Λ	The remaining performance after the performance degradation ends.	Absorption resilience
E	The time that the system remains in the postdisturbance degraded state.	Recovery resilience
Π	Slopes of performance recovery processes.	Recovery resilience
A	Area of the resilience trapezoid.	Overall resilience

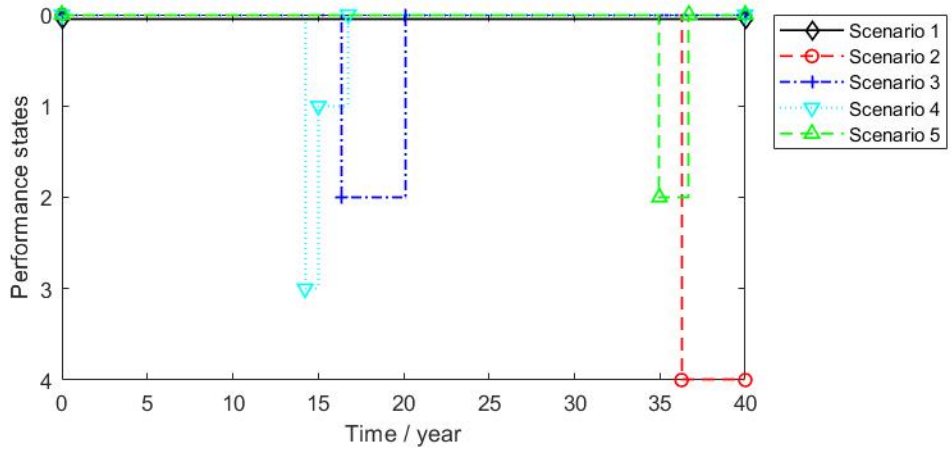

Fig. 12: *The five trajectories used to calculate the $\Phi\Lambda E\Pi$ metrics.*

It can be seen from the comparison in Figure 11 and Table XI that both the developed resilience metrics and the $\Phi\Lambda E\Pi$ metrics are able to capture different aspects of resilience. However, as shown in Table X, in the $\Phi\Lambda E\Pi$ metrics, some aspects of resilience are mixed, while the developed resilience metrics allow measuring the different aspects of resilience separately. Another major difference is that, the $\Phi\Lambda E\Pi$ metrics are defined for

TABLE XI: $\Phi\Lambda E\Pi$ *metrics.*

Scenarios	Φ (€/day)	Λ (€)	E (years)	Π (€/$year$)	A (€·$year$)
1	$--$	$--$	$--$	$--$	0
2	2.47×10^9	1.8×10^{10}	3.73	$--$	6.71×10^{10}
3	2.68×10^7	1.8×10^8	1.88	9.57×10^7	5.07×10^8
4	5.79×10^7	3.6×10^8	0.38	1.69×10^8	5.23×10^8
5	2.88×10^7	1.8×10^8	0.87	2.08×10^8	2.35×10^8

$--$: Not applicable.

individual sample paths, while the developed resilience metrics consider population characteristics. Therefore, using the developed resilience metrics could account for the variations caused by uncertainties. Compared to the $\Phi\Lambda E\Pi$ metrics, a major drawback of the developed resilience metrics is that, they cannot explicitly capture the speed of performance degradation and recovery, as the metrics Φ and Π do.

3) Time-dependent resilience analyses: In this subsection, the time-dependent behaviors of the resilience of the NPP are investigated by varying the evaluation horizon t from 0 to 80 years. The results are presented in Figure 13. It can be seen from the Figures that as the evaluation horizon increases, the resistant probability, recovery probability and overall resilience decrease. This is because the longer the NPP operates, the more likely that it is hit by an destructive earthquake. It should be noted that in the current model, the degradations of the safety systems are not considered. Therefore, the decrease of resilience with time is purely caused by the increasing likelihood of earthquake occurrences.

From Figures 13 (a) and (d), it can be seen that the resistant and overall resilience roughly decrease linearly as the evaluation horizon increases. This is because in the MRP-based resilience model, the occurrence of extreme event is modelled by a homogeneous Poisson process. For the homogeneous Poisson process, when t is small, the event occurrence probability before t can be approximated by a linear function of t [57]. The slopes of these linear decreasing functions are dependent on the reliability of the safety systems: the less reliable the safety systems, the more steep the slopes. This observation can be used by decision makers to make rough estimations and predictions of the resistant, absorption and overall resilience when necessary.

The resilient probability, as shown in Figure 13 (b), remains constant in the evaluation horizon. This is because, the safety barriers are assumed to be degradation-free. The reliabilities of the safety barriers are, therefore, constants over the evaluation horizon. As the resilient probability is determined by the reliabilities of the safety barriers, it also remains constants.

The recovery resilience, however, is a convex decreasing function of time (Figure 13 (c)): it deceases sharply first, and then becomes almost stable. This is because when t is very small, it is almost impossible to have earthquakes with large magnitudes (since their occurrence rates are too low). The damages caused by the earthquakes at this range, therefore, are also small and can be repaired in a short time. As t increases, the likelihood of having larger earthquakes with greater damages increases. Longer recovery time is, then, needed. As a consequence, the recovery resilience drops dramatically. As t further increases, the probability of entering

different performance damage states tend to stabilize. Hence, the recovery resilience also becomes stable. This finding can help the decision maker determine the optimal operation limit for the NPP. For example, Figure 13 (c) shows that, from a recovery resilience perspective, operating an NPP for 80 years is almost as good as operating it for only 30 years. Hence, if the decision maker wants to extend the life of an NPP from 30 years to 80 years, he/she does not concern about recovery resilience and only needs to look at the other three aspects of resilience.

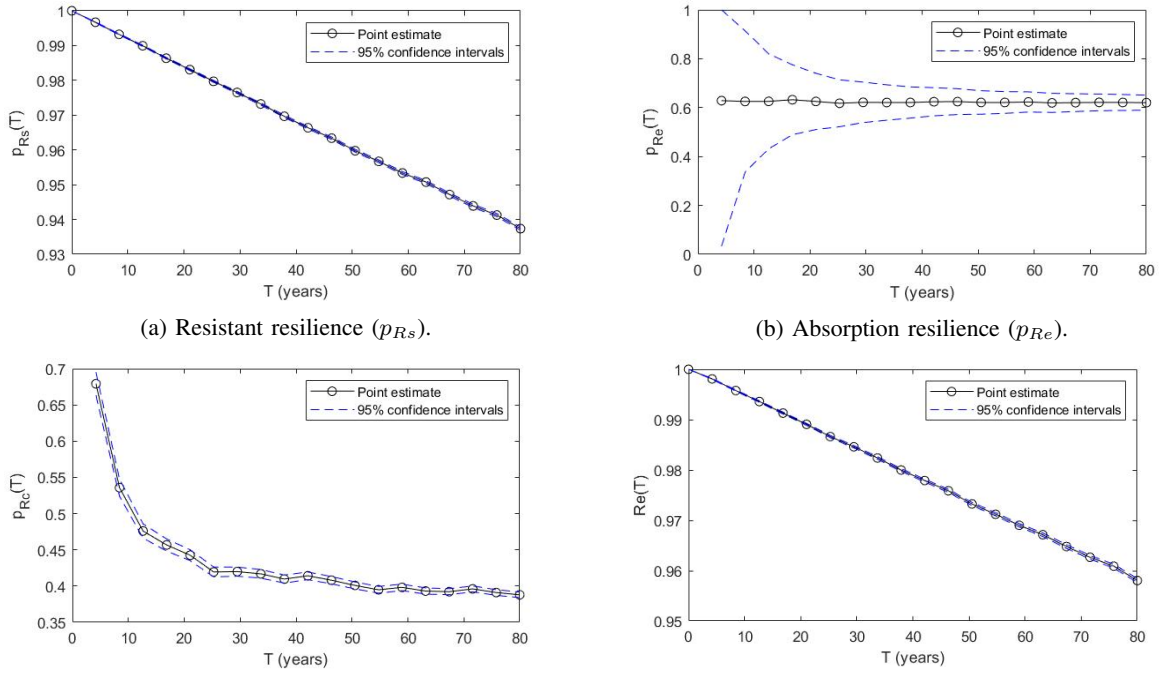

(a) Resistant resilience (p_{Rs}).

(b) Absorption resilience (p_{Re}).

(c) Recovery resilience (p_{Rc}).

(d) Overall resilience (Re).

Fig. 13: Results of the time-dependent resilience analyses.

V. Conclusion

A resilience model is developed for multistate energy systems based on Markov reward process models. In the developed model, the dynamics of system performances are modelled by a continuous time discrete state Markov chain and the losses caused by the extreme events are modeled by the reward rates associated with state sojourns or state transitions: the rewards associated with state transitions from higher-performance to lower-performance represent the direct losses caused by the extreme event; and the reward associated with sojourns in the performance degradation states represent indirect losses (*e.g.,* downtime costs). Four numerical metrics are defined to measure the three aspects of system resilience separately (resistant, absorption and recovery resilience) and collectively (overall resilience). A simulation-based algorithm is developed to support the resilience analysis.

The developed methods are applied for resilience analysis of a NPP against seismic hazards. The result of the analysis, presented as a four-dimensional radar chart, can provide a comprehensive description of the resilience

of the NPP for a given evaluation horizon. Since the developed model is able to quantify the three contributing elements to resilience (resistant, absorption and recovery capability) separately, it can also be used to plan improvement activities for the resilience. A time-dependent analysis is also conducted to investigate how does the resilience of the NPP evolves with time. The results show that in the evaluation ranges, as time goes by, the resistant, recovery and overall resilience decrease: the recovery resilience decreases dramatically at first and then converges to a constant value; while the other two resilience metrics decreases linearly with time. The absorption resilience, on the other hand, remains constant. This finding could help to make decisions regarding optimal useful life of the NPP.

Although the developed model provides an useful and efficient way for modelling and analyzing the resilience of multistate energy systems, it still has some limitations that could be improved in future researches. First, an implicit assumption of the Markov reward model is that the time-to-performance-degradation and time-to-recovery follow exponential distributions. This assumption, however, does not always hold in practice. The model can be extended to semi-Markov reward models to resolve this issue. Another drawback is that, the developed resilience analysis method is based on Monte Carlo simulation, which is computationally demanding. In the future, efforts can be made to develop analytical or semi-analytical analysis methods for resilience analysis, in order to reduce the computational burden.

ACKNOWLEDGMENT

This work was finished during Dr. Shijia Du's visit to Université Paris-Saclay. She would like to express her deepest gratitude to Professor Enrico Zio for hosting her visit. Dr. Du's research is supported by Natural Science Foundation of China (NSFC) under grant No. 71601010. The work in this paper is also partially supported by High-end Foreign Experts Recruitment Program of Shanghai university, China (July - August, 2019).

REFERENCES

[1] F. H. Jufri, V. Widiputra, and J. Jung, "State-of-the-art review on power grid resilience to extreme weather events: Definitions, frameworks, quantitative assessment methodologies, and enhancement strategies," *Applied Energy*, vol. 239, pp. 1049–1065, 2019.

[2] W. House, "Economic benefits of increasing electric grid resilience to weather outages," *Washington, DC: Executive Office of the President*, 2013.

[3] Z. Bie, Y. Lin, G. Li, and F. Li, "Battling the extreme: A study on the power system resilience," *Proceedings of the IEEE*, vol. 105, no. 7, pp. 1253–1266, 2017.

[4] S. Hosseini, K. Barker, and J. E. Ramirez-Marquez, "A review of definitions and measures of system resilience," *Reliability Engineering & System Safety*, vol. 145, pp. 47–61, 2016.

[5] Z. Zeng, S. Du, and Y. Ding, "Resilience analysis of multi-state systems with time-dependent behaviors," *Applied Mathematical Modelling*, vol. 90, pp. 889–911.

[6] M. Rahnamay-Naeini, Z. Y. Wang, N. Ghani, A. Mammoli, and M. M. Hayat, "Stochastic analysis of cascading-failure dynamics in power grids," *Ieee Transactions on Power Systems*, vol. 29, no. 4, pp. 1767–1779, 2014.

[7] J. Ma, S. X. Wang, Y. Qiu, Y. N. Li, Z. P. Wang, and J. S. Thorp, "Angle stability analysis of power system with multiple operating conditions considering cascading failure," *Ieee Transactions on Power Systems*, vol. 32, no. 2, pp. 873–882, 2017.

[8] M. Sanghavi, S. Tadepalli, T. J. Boyle, M. Downey, and M. K. Nakayama, "Efficient algorithms for analyzing cascading failures in a markovian dependability model," *Ieee Transactions on Reliability*, vol. 66, no. 2, pp. 258–280, 2017.

[9] Y. X. Liu, Y. Wang, P. Yong, N. Zhang, C. Q. Kang, and D. Lu, "Fast power system cascading failure path searching with high wind power penetration," *Ieee Transactions on Sustainable Energy*, vol. 11, no. 4, pp. 2274–2283, 2020.

[10] A. Reibman, R. Smith, and K. Trivedi, "Markov and markov reward model transient analysis: An overview of numerical approaches," *European Journal of Operational Research*, vol. 40, no. 2, pp. 257–267, 1989.

[11] "Critical infrastructure resilience: Final report and recommendations," tech. rep., National Infrastructure Advisory Council, 2009.

[12] C. S. Holling, "Resilience and stability of ecological systems," *Annual review of ecology and systematics*, vol. 4, no. 1, pp. 1–23, 1973.

[13] A. Pregenzer, "Systems resilience: a new analytical framework for nuclear nonproliferation," *Albuquerque, NM: Sandia National Laboratories*, 2011.

[14] B. Allenby and J. Fink, "Social and ecological resilience: toward inherently secure and resilient societies," *Science*, vol. 24, no. 3, pp. 347–364, 2000.

[15] E. Hollnagel, D. D. Woods, and N. Leveson, *Resilience engineering: Concepts and precepts*. Ashgate Publishing, Ltd., 2006.

[16] Y. Sheffi, D. Closs, J. Davidson, D. French, B. Gordon, R. Martichenko, J. Mentzer, C. Norek, N. Seiersen, and T. Stank, "Supply chain resilience how can you transcend vulnerability in your supply chain to gain competitive advantage," *The Official Magazine of The Logistics Institute*, vol. 12, no. 1, pp. 12–17, 2006.

[17] B. J. Pfefferbaum, D. B. Reissman, R. L. Pfefferbaum, R. W. Klomp, and R. H. Gurwitch, "Building resilience to mass trauma events," in *Handbook of injury and violence prevention*, pp. 347–358, Springer, 2008.

[18] I. Iervolino and M. Giorgio, "Stochastic modeling of recovery from seismic shocks," in *12th International Conference on Applications of Statistics and Probability in Civil Engineering*, pp. 12–15, 2015.

[19] Y. Y. Haimes, "On the definition of resilience in systems," *Risk Analysis: An International Journal*, vol. 29, no. 4, pp. 498–501, 2009.

[20] I. S. P. (Organization), *Regional disaster resilience: A guide for developing an action plan*. DIANE

Publishing Inc., 2006.

[21] E. D. Vugrin, D. E. Warren, M. A. Ehlen, and R. C. Camphouse, "A framework for assessing the resilience of infrastructure and economic systems," in *Sustainable and resilient critical infrastructure systems*, pp. 77–116, Springer, 2010.

[22] Y. Sheffi *et al.*, "The resilient enterprise: overcoming vulnerability for competitive advantage," *MIT Press Books*, vol. 1, 2005.

[23] R. Westrum, "A typology of resilience situations," in *Resilience engineering*, pp. 67–78, CRC Press, 2017.

[24] M. Bruneau, S. E. Chang, R. T. Eguchi, G. C. Lee, T. D. O'Rourke, A. M. Reinhorn, M. Shinozuka, K. Tierney, W. A. Wallace, and D. Von Winterfeldt, "A framework to quantitatively assess and enhance the seismic resilience of communities," *Earthquake spectra*, vol. 19, no. 4, pp. 733–752, 2003.

[25] A. Rose, "Economic resilience to natural and man-made disasters: Multidisciplinary origins and contextual dimensions," *Environmental Hazards*, vol. 7, no. 4, pp. 383–398, 2007.

[26] C. W. Zobel and L. Khansa, "Characterizing multi-event disaster resilience," *Computers & Operations Research*, vol. 42, pp. 83–94, 2014.

[27] M. Panteli, D. N. Trakas, P. Mancarella, and N. D. Hatziargyriou, "Power systems resilience assessment: Hardening and smart operational enhancement strategies," *Proceedings of the IEEE*, vol. 105, no. 7, pp. 1202–1213, 2017.

[28] D. Henry and J. E. Ramirez-Marquez, "Generic metrics and quantitative approaches for system resilience as a function of time," *Reliability Engineering & System Safety*, vol. 99, pp. 114–122, 2012.

[29] M. Amirioun, F. Aminifar, H. Lesani, and M. Shahidehpour, "Metrics and quantitative framework for assessing microgrid resilience against windstorms," *International Journal of Electrical Power & Energy Systems*, vol. 104, pp. 716–723, 2019.

[30] S. E. Chang and M. Shinozuka, "Measuring improvements in the disaster resilience of communities," *Earthquake spectra*, vol. 20, no. 3, pp. 739–755, 2004.

[31] M. Ouyang, L. Dueñas-Osorio, and X. Min, "A three-stage resilience analysis framework for urban infrastructure systems," *Structural safety*, vol. 36, pp. 23–31, 2012.

[32] J. Wang, W. Zuo, L. Rhode-Barbarigos, X. Lu, J. Wang, and Y. Lin, "Literature review on modeling and simulation of energy infrastructures from a resilience perspective," *Reliability Engineering & System Safety*, 2018.

[33] D. L. Alderson, G. G. Brown, and W. M. Carlyle, "Assessing and improving operational resilience of critical infrastructures and other systems," in *Bridging Data and Decisions*, pp. 180–215, Informs, 2014.

[34] S. D. Manshadi and M. E. Khodayar, "Resilient operation of multiple energy carrier microgrids," *IEEE Transactions on Smart Grid*, vol. 6, no. 5, pp. 2283–2292, 2015.

[35] C. Chen, J. Wang, F. Qiu, and D. Zhao, "Resilient distribution system by microgrids formation after natural disasters," *IEEE Transactions on smart grid*, vol. 7, no. 2, pp. 958–966, 2016.

[36] W. Yuan, J. Wang, F. Qiu, C. Chen, C. Kang, and B. Zeng, "Robust optimization-based resilient distribution network planning against natural disasters," *IEEE Transactions on Smart Grid*, vol. 7, no. 6, pp. 2817–2826, 2016.

[37] Y. Fang, N. Pedroni, and E. Zio, "Optimization of cascade-resilient electrical infrastructures and its validation by power flow modeling," *Risk Analysis*, vol. 35, no. 4, pp. 594–607, 2015.

[38] J. Page, D. Basciotti, O. Pol, J. N. Fidalgo, M. Couto, R. Aron, A. Chiche, and L. Fournié, "A multi-energy modeling, simulation and optimization environment for urban energy infrastructure planning," in *Proceedings of the 13th conference of international building performance simulation association, Chambéry, France*, pp. 26–28, 2013.

[39] G. Chen, Z. Y. Dong, D. J. Hill, G. H. Zhang, and K. Q. Hua, "Attack structural vulnerability of power grids: A hybrid approach based on complex networks," *Physica A: Statistical Mechanics and its Applications*, vol. 389, no. 3, pp. 595–603, 2010.

[40] X. Liu, E. Ferrario, and E. Zio, "Resilience analysis framework for interconnected critical infrastructures," *ASCE-ASME Journal of Risk and Uncertainty in Engineering Systems, Part B: Mechanical Engineering*, vol. 3, no. 2, p. 021001, 2017.

[41] M. Panteli and P. Mancarella, "Modeling and evaluating the resilience of critical electrical power infrastructure to extreme weather events," *IEEE Systems Journal*, vol. 11, no. 3, pp. 1733–1742, 2017.

[42] F. Cadini, G. L. Agliardi, and E. Zio, "A modeling and simulation framework for the reliability/availability assessment of a power transmission grid subject to cascading failures under extreme weather conditions," *Applied energy*, vol. 185, pp. 267–279, 2017.

[43] G. Li, P. Zhang, P. B. Luh, W. Li, Z. Bie, C. Serna, and Z. Zhao, "Risk analysis for distribution systems in the northeast us under wind storms," *IEEE Transactions on Power Systems*, vol. 29, no. 2, pp. 889–898, 2014.

[44] R. Rocchetta, E. Zio, and E. Patelli, "A power-flow emulator approach for resilience assessment of repairable power grids subject to weather-induced failures and data deficiency," *Applied energy*, vol. 210, pp. 339–350, 2018.

[45] E. Ferrario and E. Zio, "Goal tree success tree–dynamic master logic diagram and monte carlo simulation for the safety and resilience assessment of a multistate system of systems," *Engineering Structures*, vol. 59, pp. 411–433, 2014.

[46] Z. Zeng and E. Zio, "An integrated modeling framework for quantitative business continuity assessment," *Process Safety and Environmental Protection*, vol. 106, pp. 76–88, 2017.

[47] B. D. Youn, C. Hu, and P. Wang, "Resilience-driven system design of complex engineered systems," *Journal of Mechanical Design*, vol. 133, no. 10, p. 101011, 2011.

[48] T. Hashimoto, J. R. Stedinger, and D. P. Loucks, "Reliability, resiliency, and vulnerability criteria for water resource system performance evaluation," *Water resources research*, vol. 18, no. 1, pp. 14–20, 1982.

[49] Y.-F. Li and E. Zio, "A multi-state model for the reliability assessment of a distributed generation system via universal generating function," *Reliability Engineering & System Safety*, vol. 106, pp. 28–36, 2012.

[50] H. Nabli and B. Sericola, "Performability analysis: a new algorithm," *IEEE Transactions on Computers*, vol. 45, no. 4, pp. 491–494, 1996.

[51] T. Anagnos and A. S. Kiremidjian, "A review of earthquake occurrence models for seismic hazard analysis," 1988.

[52] P. Todorovic and E. Zelenhasic, "A stochastic model for flood analysis," *Water Resources Research*, vol. 6, no. 6, pp. 1641–1648, 1970.

[53] R. W. Katz, "Stochastic modeling of hurricane damage," *Journal of Applied Meteorology*, vol. 41, no. 7, pp. 754–762, 2002.

[54] J. W. Baker, "An introduction to probabilistic seismic hazard analysis," *White paper, version*, vol. 1, p. 72, 2008.

[55] R. E. Barlow and F. Proschan, *Mathematical theory of reliability*, vol. 17. Siam, 1996.

[56] M. Fan, Z. Zeng, E. Zio, and R. Kang, "Modeling dependent competing failure processes with degradation-shock dependence," *Reliability Engineering & System Safety*, vol. 165, pp. 422–430, 2017.

[57] S. M. Ross, *Introduction to probability models*. Academic press, 2014.

[58] "Earthquake preparedness and response for nuclear power plants," tech. rep., International Atomic Energy Agency (IAEA), 2011.

[59] "The international nuclear and radiological event scale," tech. rep., International Atomic Energy Agency (IAEA), 2008.

[60] E. Zio and E. Ferrario, "A framework for the system-of-systems analysis of the risk for a safety-critical plant exposed to external events," *Reliability Engineering & System Safety*, vol. 114, pp. 114–125, 2013.

[61] R. Kassawara *et al.*, "Seismic probabilistic risk assessment implementation guide," tech. rep., EPRI, No1002989, 2003.

[62] C. A. Cornell, H. Banon, and A. F. Shakal, "Seismic motion and response prediction alternatives," *Earthquake Engineering & Structural Dynamics*, vol. 7, no. 4, pp. 295–315, 1979.

[63] "Gutenberg-richter relationship: Magnitude vs. frequency of occurrence." https://www.eoas.ubc.ca/courses/eosc256/Feb7_2011_GR.pdf. Accessed: 2019-05-06.

[64] L. Chen, "Safety of Nuclear Energy: Analysis of Events at Commercial Nuclear Power Plants," Master's thesis, ETH Zurich, Switzerland, 2018.

[65] "Electricity price statistics." https://ec.europa.eu/eurostat/statistics-explained/index.php/Electricity_price_statistics. Accessed: 2019-04-22.